Plant Physiology and Biochemistry 143 (2019) 375–387

Contents lists available at ScienceDirect

Plant Physiology and Biochemistry

journal homepage: www.elsevier.com/locate/plaphy

Research article

Constitutive expression of chloroplast glycerol-3-phosphate acyltransferase from *Ammopiptanthus mongolicus* enhances unsaturation of chloroplast lipids and tolerance to chilling, freezing and oxidative stress in transgenic Arabidopsis

Min Xue, Ting Guo, Meiyan Ren, Zhilin Wang, Kuangang Tang, Wenjun Zhang, Maoyan Wang*

College of Life Sciences, Inner Mongolia Agricultural University, No. 306 Zhaowuda Street, Hohhot, 010018, China

ARTICLE INFO

Keywords:
Ammopiptanthus mongolicus
Glycerol-3-phosphate acyltransferase
Phosphatidylglycerol
Temperature stress
Oxidative stress

ABSTRACT

Chloroplast glycerol-3-phosphate acyltransferase (GPAT) is the first key enzyme determining the unsaturation of phosphatidylglycerol (PG) in thylakoid membranes and is involved in the tolerance of plants to chilling, heat and high salinity. However, whether the GPAT affects plant tolerance to other stressors has been scarcely reported. *Ammopiptanthus mongolicus* is the only evergreen broadleaf shrub growing in the central Asian desert, and it has a high tolerance to harsh environments, especially extreme cold. This study aimed to characterize the physiological function of *AmGPAT* from *A. mongolicus*. The transcription of *AmGPAT* was markedly induced by cold and drought but differentially suppressed by heat and high salinity in the laboratory-cultured seedlings. The gene also had the highest transcription levels in the leaves of shrubs naturally growing in the wild during the late autumn and winter months throughout the year. Moreover, *AmGPAT* was most abundantly expressed in leaves and immature pods rather than other organs of the shrubs. Constitutive expression of *AmGPAT* in Arabidopsis increased the levels of *cis*-unsaturated fatty acids, especially that of linolenic acid (18:3), mainly in PG but also in other chloroplast lipids in transgenic lines. More importantly, the transgene significantly increased the tolerance of the transgenics not only to chilling but also to freezing and oxidative stress at both the cellular and whole-plant levels. In contrast, this gene reduced heat tolerance of the transgenic plants. This study improves the current understanding of chloroplast GPAT in plant tolerance against abiotic stressors through regulating the unsaturation of chloroplast lipids, mainly that of PG.

1. Introduction

Cold stress, which includes chilling (0–15 °C) and freezing (< 0 °C) temperatures, is a major factor limiting the geographical distribution of plant species and the growth and yield of crop plants worldwide (Shi et al., 2018). At the cellular level, membranes, especially those enclosing chloroplasts, thylakoids and the cell itself, are known to be the primary sites of cold injury (Kratsch and Wise, 2000; Heidarvand and Amiri, 2010). Chilling stress usually causes a decrease in membrane fluidity and membrane protein activity and therefore disturbs the physiological functions of cells. By contrast, freezing temperatures generally result in severe cellular dehydration and ice crystal formation around and/or inside cells, which may lead to the disruption of cellular membranes and/or cell death (Heidarvand and Amiri, 2010; Shi et al., 2018). Plants have evolved corresponding mechanisms to maintain appropriate fluidity and integrity of cellular membranes under low temperatures. One such mechanism is the modification of membrane lipid composition, particularly an increase in the level of *cis*-unsaturated fatty acids [UFAs; including oleic acid (18:1), linoleic acid (18:2) and linolenic acid (18:3)] in phosphatidylglycerol (PG) during cold acclimation (Tamada et al., 2004; Upchurch, 2008).

Phosphatidylglycerol is the only phospholipid in thylakoid membranes of chloroplasts in higher plants, and its synthesis is initiated by the glycerol-3-phosphate (G-3-P) acyltransferase (GPAT, EC 2.3.1.15) localized in chloroplast stroma (Wallis and Browse, 2002; Wada and Murata, 2007; Chen et al., 2011). The enzyme transfers an acyl chain to the *sn*-1 position of G-3-P to generate lysophosphatidic acid (LPA). Then, the palmitoyl (16:0) acyl chain is exclusively esterified at the *sn*-2 position of the LPA to produce phosphatidic acid (PA). This PA is used for the synthesis of PG or is converted to other major chloroplast

* Corresponding author.
E-mail addresses: xuemin808@126.com (M. Xue), 735516773@qq.com (T. Guo), meiyanren@126.com (M. Ren), wangzlnm@163.com (Z. Wang), tangkuangang@163.com (K. Tang), 1392344739@qq.com (W. Zhang), wangmaoyan@163.com (M. Wang).

https://doi.org/10.1016/j.plaphy.2019.07.019
Received 19 February 2019; Received in revised form 19 July 2019; Accepted 19 July 2019
Available online 20 July 2019
0981-9428/

Abbreviations

ACP	acyl carrier protein
cTP	chloroplast targeting peptide
DAB	3,3′-diaminobenzidine
DBI	double bond index
DGDG	digalactosyldiacylglycerol
D/NATs	day/night air temperatures
2D-TLC	two-dimensional thin-layer chromatography
FAME	fatty acid methyl ester
GGGT	galactolipid: galactolipid galactosyltransferase
G-3-P	glycerol-3-phosphate
GPAT	glycerol-3-phosphate acyltransferase
H_{II}	hexagonal II
H_2O_2	hydrogen peroxide
LPA	lysophosphatidic acid
LPO	lipid peroxidation
MDA	malondialdehyde
MGDG	monogalactosyldiacylglycerol
MS	Murashige and Skoog
ORF	open reading frame
PA	phosphatidic acid
PG	phosphatidylglycerol
PPT	phosphinothricin
PSII	photosystem II
REC	relative electrical conductivity
ROS	reactive oxygen species
RT-qPCR	real-time quantitative PCR
SD	standard deviation
SQDG	sulfoquinovosyldiacylglycerol
UFA	unsaturated fatty acid
WT	wild type

membrane lipids, namely monogalactosyldiacylglycerol (MGDG), digalactosyldiacylglycerol (DGDG) and sulfoquinovosyldiacylglycerol (SQDG), via diacylglycerol in chloroplasts (Wallis and Browse, 2002; Wada and Murata, 2007). Previous studies have shown that the GPATs from cold-tolerant plants, such as Arabidopsis (*Arabidopsis thaliana*) and spinach (*Spinacia oleracea*), prefer 18:1 to 16:0 acyl chain as a substrate, while those from cold-sensitive plants such as squash (*Cucurbita moschata*) and *Amaranthus lividus* mostly utilize these two substrates at comparable rates or display a higher activity with 16:0 than with 18:1 (Ariizumi et al., 2002; Sakamoto et al., 2003; Wada and Murata, 2007; Chen et al., 2011). The 18:1 at the *sn*-1 position can be further desaturated into 18:2 and then 18:3, while the 16:0 at this position generally remains unchanged. The 16:0 acyl chain at the *sn*-2 position can be frequently desaturated to *trans*-3-hexadecenoic acid (16:1*t*) in all plants (Wada and Murata, 2007). Thus, cold-tolerant plants commonly have a larger proportion of 18-C UFAs in the PG compared to cold-sensitive plants, which is believed to correlate with a low phase transition temperature of thylakoid membranes and thus helps to maintain the fluidity, integrity and functioning of the membranes under chilling stress (Tamada et al., 2004; Upchurch, 2008). Naturally, the GPAT enzyme has been regarded as a key regulator of plant chilling tolerance.

Except for the gene encoding soluble chloroplast GPAT (ATS1) that uses acyl carrier protein (ACP) as its acyl donor, nine other *GPAT* genes, *AtGPAT1* to *AtGPAT9*, have been identified in the genome of Arabidopsis. All the nine *AtGPATs* have been confirmed to encode mitochondria-membrane targeted enzymes (AtGPAT1 to AtGPAT3) or endoplasmic reticulum-bound enzymes (AtGPAT4 to AtGPAT9) that are known to use acyl-coenzyme A and acyl-ACP as their natural acyl substrates (Waschburger et al., 2018). These membrane-bound AtGPATs have been documented to be mainly involved in the biosyntheses of membrane lipids, storage lipids, and/or extracellular lipid polyesters such as cutin or suberin (Chen et al., 2011; Waschburger et al., 2018).

Functional characterization of Arabidopsis chloroplast GPAT gene (*ATS1*) was based on the identification of its mutant lines *ats1s* that exhibited a reduction in PG and C16 fatty acid contents but had no obvious alteration in phenotypes (Xu et al., 2006). The genes for chloroplast GPAT have also been identified in many other plant species, and several have been functionally characterized, including those from squash, spinach, tomato (*Lycopersicon esculentum*), sweet pepper (*Capsicum annuum*) and *Suaeda salsa* (Murata et al., 1992; Ariizumi et al., 2002; Sakamoto et al., 2003; Sui et al., 2007c, 2017; Yan et al., 2008; Sun et al., 2011; Ivanov et al., 2012). A few of these genes were shown to be induced by cold and/or high salinity but suppressed by heat, drought, salt and abscisic acid treatments (Sui et al., 2007c, 2017; Gupta et al., 2013; Sun et al., 2015; Li et al., 2018). Overexpressing the *GPATs* from cold-tolerant Arabidopsis and spinach increased the UFA level of the leaf PG and concomitantly improved the photosynthesis and growth of their transgenic plants during chilling treatments (Murata et al., 1992; Yokoi et al., 1998; Ariizumi et al., 2002). In contrast, overexpressing the *GPATs* from cold-sensitive squash and sweet pepper enhanced the saturation level of the PG and chilling sensitivity or thermotolerance of the photosynthetic apparatus and growth of transgenic plants (Murata et al., 1992; Sakamoto et al., 2003; Yan et al., 2008; Ivanov et al., 2012). Unexpectedly, overexpressing *LeGPAT* in tomato that is sensitive to chilling also increased the PG unsaturation and chilling tolerance of the photosynthetic apparatus through the selective preference of the LeGPAT enzyme for 18:1 over 16:0 (Sui et al., 2007a, 2007c; Sun et al., 2011). Furthermore, both *LeGPAT* and *SsGPAT* from *S.salsa*, a typical saline-alkaline indicator plant, could improve salt tolerance of transgenic plants (Sun et al., 2010; Sui et al., 2017). However, whether chloroplast GPAT gene affects the tolerance of plants to drought, freezing and oxidative stress that is caused by the overproduced reactive oxygen species (ROS) under various abiotic stresses (Gill and Tuteja, 2010) remains unknown or has been scarcely reported. It is necessary to investigate these aspects of the *GPATs* from more plant species, especially those with high stress tolerance.

Ammopiptanthus mongolicus (Maxim. ex kom.) Cheng F. is an endangered survivor from the Tethys in the Tertiary Period and is the only evergreen broadleaf shrub plant growing in the central Asian desert. This species can tolerate extremely cold weather (as low as approximately −30 °C during winters), intense ultraviolet irradiation, and a very dry climate (Wu et al., 2014; Yin et al., 2018). Given its ancient origin and unique capacity to survive in harsh environments, *A. mongolicus* likely evolved special molecular mechanisms to protect its photosynthetic apparatus and cellular membranes against abiotic stressors, especially cold. However, reports about this aspect of *A. mongolicus* are lacking. In our previous study, a full-length cDNA sequence for chloroplast GPAT (*AmGPAT*) was identified in the *A. mongolicus* transcriptome (Wu et al., 2014). In the present study, we isolated the cDNA and investigated its roles in response and tolerance to cold and other abiotic stressors. The gene exhibited an obvious negative correlation at the transcriptional level with the stress temperatures imposed in both the laboratory and natural field conditions. Constitutive expression of *AmGPAT* in Arabidopsis not only substantially increased the UFA level in PG and chilling tolerance but also improved the endurance to freezing and oxidative stress of transgenic plants. These results improve the current understanding of the physiological roles of chloroplast GPAT in plant stress tolerance and provide new evidence of the potential effects of *AmGPAT* on the ability of *A. mongolicus* shrubs to endure seasonal cold weather and intense ultraviolet irradiation or oxidative stress in the wild.

2. Materials and methods

2.1. Stress treatments and field sampling of A. mongolicus

Ripe seeds were collected from *A. mongolicus* shrubs naturally growing in the southern suburb of Hohhot (40°51′N, 110°46′E), Inner Mongolia, China. The seeds were surface sterilized and cultured in pots filled with sand under normal conditions as described previously (Wu et al., 2014). At 1.5 months after the planting date, the seedlings were exposed to cold, heat, salt or drought treatment as described by Yin et al. (2018). Briefly, the cold treatment was performed in a low-temperature programmable incubator (Percival, LT-36VL, USA) with gradual cooling: 4 °C for the first 24 h, 0 °C for the next 12 h, and −6 °C for the last 12 h under dim light of ~100 μmol•m^{-2}•s^{-1} (the same light level was used for all dim lighting below). For the heat treatment, seedlings in pots were incubated at 42 °C in the dark for 48 h in an electric incubator (UF110, Memmert, Germany); the seedlings were watered every 8 h to avoid drought stress. For the salt treatment, seedlings were watered once with a 350 mM NaCl solution (Yin et al., 2018). After initiation of the cold, heat or salt treatment, seedlings were carefully removed from their pots at 2, 6, 12, 24 or 48 h and washed with tap water before being collected. Salt treatment was also conducted by watering seedlings with a 50 mM NaCl solution on the first day and the concentration was increased by 50 mM NaCl on each subsequent day until the final concentration was reached to 100, 200 or 300 mM NaCl (Sui et al., 2017). Two weeks later, the treated seedlings were sampled. Drought treatment was carried out by suspending watering of the seedlings for 14 d, and the seedlings were sampled after 4, 6, 8, 10, 11, 12, 13 and 14 d from the beginning of the treatment period. For each treatment, seedlings sampled at 0 h or on day 0 (unstressed) were used as controls.

Organ samples were collected for gene expression analysis from the *A. mongolicus* shrubs naturally growing in the southern suburb of Hohhot, Inner Mongolia, China. For the expression analysis by month, young leaves of the shrubs were sampled on one morning at the beginning of each month from July 2016 to June 2017. For the expression analysis by plant organ, young leaves, young twigs, lateral roots and flower buds were sampled in late April 2017, and immature pods were sampled in early June 2017.

All samples taken from the laboratory-grown seedlings and the naturally growing shrubs were immediately frozen in liquid nitrogen and then stored at −76 °C before RNA extraction.

2.2. Gene cloning and protein prediction

Total RNAs of the stored (−76 °C) plant samples were isolated using a modified TRIzol method as described earlier and were purified with RQI RNase-Free DNase (Promega, USA) (Wu et al., 2014). First-strand cDNAs were synthesized from the purified RNAs using Moloney murine leukemia virus reverse transcriptase (Promega, USA). The open reading frame (ORF) cDNA of *AmGPAT* was amplified by PCR from the cDNA sample of *A. mongolicus* seedlings using the primer pair 5′-GTGTCTAGAGGGAGAATCGGTATTACC-3′ (forward primer including the restriction enzyme *Xba*I recognition site) and 5′-GGTCCCGGGTCATCAGAGCAAAGTATA-3′ (reverse primer including the restriction enzyme *Sma*I recognition site). The cDNA fragment was cloned into a pMD19-T vector (Takara Biotech, Dalian, China) and then sequenced.

The physicochemical properties of the deduced AmGPAT protein were predicted using various software programs. The transit peptide and subcellular localization of the protein were predicted using the online programs ChloroP 1.1 Server (http://www.cbs.dtu.dk/services/ChloroP/) and ProtComp v9.0 (http://linux1.softberry.com/berry.phtml?topic=protcomppl&group=programs&subgroup=proloc), respectively. Functional domains and classification were predicted using SMART online software (http://smart.embl-heidelberg.de/). Multiple alignments of full-length GPAT sequences were performed with ClustalW. The phylogenetic tree was constructed using the Neighbor-joining (NJ) method and bootstrap analysis of 1000 replicates in MEGA 7.0 software.

2.3. Real-time quantitative PCR

Fluorescent real-time quantitative PCR (RT-qPCR) was used to detect the expression patterns of *AmGPAT* in *A. mongolicus*. The first-strand cDNAs described in Section 2.2 were diluted 10-fold with deionized water and were used as templates for the PCR. *AmeIF1* was used as an internal reference gene and was amplified using the following respective forward and reverse primer pair: 5′-CTGACATGCGCCGTAGGAACG-3′ and 5′-CCCTGCTTATGCCAGTCTTTT-3′. The primer pair for *AmGPAT* consisted of 5′-AAGAGAGAGCCTTTTGACTACTACAT-3′ (forward) and 5′-TCTGCTTCCGTTTGGTGATTT-3′ (reverse). The reactions for RT-qPCR were performed using 2 × SYBR Green PCR Master Mix (Takara, Japan) and a LightCycler 480 system (Roche, Germany). The reactions were subjected to an initial denaturation step of 95 °C for 1 min followed by 40 cycles of 95 °C for 15 s, 61 °C for 20 s and 72 °C for 30 s, after which one cycle of 95 °C for 15 s followed by 61 °C for 1 min was performed. The relative expression levels were calculated using the $2^{-\Delta\Delta Ct}$ method (Livak and Schmittgen, 2001).

2.4. Generation and confirmation of transgenic Arabidopsis

The cDNA ORF fragment of *AmGPAT* was subcloned downstream of a CaMV 35S promoter in a pCAMBIA3300-35ST (p3300-35ST) vector containing a selectable marker gene for phosphinothricin (PPT). The recombinant plasmid (p3300:35S-*AmGPAT*) was subsequently introduced into *Agrobacterium tumefaciens* cells (GV3101 strain). The Arabidopsis plants (ecotype Columbia 0) grown in pots with a mixture of nutrient soil/vermiculite (1/1, v/v) under normal growth conditions (22 °C under a 16-h light/8-h dark cycle at ~150 μmol · m^{-2} · s^{-1}) were transformed by the *A. tumefaciens*-mediated floral dip method. The T_1 transgenic plants were confirmed by PPT (0.5‰, v/v) screening and PCR detection using the primer pair specific for the amplification of the *AmGPAT* ORF. The T_2 transgenic lines that exhibited an approximate 3:1 segregation ratio of green: white seedlings on 1/2 Murashige and Skoog (MS) agar plates containing 7 mg · L^{-1} PPT were estimated to harbor a single copy of *AmGPAT* and used to perform a semi-quantitative RT-PCR analysis of the transgene (*AtACTIN2* served as an internal reference gene). The homozygous T_3 lines (producing 100% green seedlings on 1/2 MS agar plates containing 7 mg · L^{-1} PPT) were used for subsequent experiments.

2.5. Lipid extraction and analysis

Lipids were extracted from the leaves of one-month-old Arabidopsis plants as described by Siegenthaler and Eichenberger (1984), and further experiments were performed according to previous methods (Xu and Siegenthaler, 1997; Botella et al., 2016). Lipid classes were separated on silica gel plates by two-dimensional thin-layer chromatography (2D-TLC). The first solvent was chloroform/methanol/water (65/25/4, v/v), and the second was chloroform/methanol/ammonia water (65/35/5, v/v). The spots of lipids were visualized under UV light by exposure to 0.01% (w/v) primuline in 60% (v/v) acetone. Then the individual lipids were scraped off from the 2D-TLC plates and collected into tubes, which were then added 5% H_2SO_4 in methanol and sat for 1 h at 85 °C to prepare fatty acid methyl esters (FAMEs). Heptadecylic acid (17:0; Sigma, USA) was added as an internal standard before methylation to quantify FAMEs. FAMEs were separated using a gas chromatograph (7890A; Agilent, Santa Clara, USA) equipped with a DB23 capillary column (60 m × 0.25 mm × 0.25 μm). Samples and standards [37 component FAMEs mix, ANPEL, China; methyl 7(Z), 10(Z)-hexadecadienoate, Larodan, Sweden; methyl 7(Z), 10(Z), 13(Z)-hexadecatrienoate, Larodan, Sweden] were injected in a split ratio of

1:10. Nitrogen was used as the carrier gas with a linear rate of 1.0 mL · min^{-1}.The column oven temperature was initially held at 120 °C for 5 min, then raised to 180 °C at a rate of 10 °C · min^{-1}, and finally to 230 °C at 2 °C · min^{-1} and maintained for 5 min. FAMEs were identified by comparison of their retention times with those of standards and quantified by the measurement of peak areas using 17:0 for calibration. The relative contents of the lipids were estimated from the amounts of fatty acids of each lipid class (Xu and Siegenthaler, 1997; Botella et al., 2016). The double bond index (DBI) was calculated as follows: DBI = Σ(mol% fatty acid content × number of double bonds). For each measurement, at least five plants were used as a source of leaf material for lipid extraction and analysis.

2.6. Stress tolerance analysis of transgenic Arabidopsis

Transgenic lines and wild type (WT) Arabidopsis (used as a control) grown in pots were cultured in a growth chamber under normal growth conditions as described above for approximately two weeks. Then, the seedlings were used to perform temperature stress tolerance assays.

For the chilling tolerance experiments, two-week-old seedlings were placed in the same incubator as described above. The seedlings were treated with a temperature of 8 °C under a 14-h light/10-h dark cycle in dim light for two weeks, after which they were returned to their previous normal growth conditions for recovery. The fresh weights and plant heights of the aerial parts of each plant line were measured after two weeks of recovery. Freezing tolerance tests were also carried out independently in the same incubator. Two-week-old seedlings were exposed to −6 °C for 8 h in dim light after a pre-treatment at 4 °C for 24 h in dim light and a post-treatment at 4 °C for 12 h in dim light again. Then, the seedlings were returned to their previous normal growth conditions to recover from the stress. The survival rates and plant heights of all the stress-treated plants were measured after two weeks and four weeks of recovery, respectively. Heat stress tolerance was analyzed by pretreating the 18-day-old seedlings with 37 °C for 2 h in the same electric incubator as described above, after which the seedlings were returned to their previous normal growth conditions for recovery for 2 h; lastly, they were exposed to 54 °C for 2 h. To avoid drought stress during the pretreatment and final heat shock periods, the pots with seedlings were placed in a plastic tray that contained water. The fresh weights of the aerial parts and siliques of each plant line were measured on the 28th day after the stress-treated seedlings were returned to normal growth conditions for recovery.

Oxidative stress tolerance was tested at the seed germination stage under high concentrations of exogenous hydrogen peroxide (H_2O_2). The sterilized seeds of WT and transgenic lines were sown on 1/2 MS agar plates (as a control) or 1/2 MS agar plates with 1.0 or 4.0 mM H_2O_2. The plates were maintained at 4 °C for 3 d and then moved to the same normal growth conditions in which the potted seedlings were cultured. The germination rates (emergence of green cotyledons) and fresh weights (20 seedlings) of each plant line were measured on the 8th day of the incubation period.

2.7. Measurement of chlorophyll fluorescence

The maximal photochemical efficiency of photosystem II (PSII; Fv/Fm) was measured to reflect photoinhibition. One-month-old transgenic and WT plants grown in pots under normal growth conditions were exposed to 6 °C for 10 h under an illumination of 600 μmol · m^{-2} · s^{-1} and then returned to their previous normal growth conditions for recovery. After 5 h or 10 h of the chilling treatment and 8 h, 18 h or 30 h of the recovery period, chlorophyll fluorescence of the fourth to eighth rosette leaves was measured with a portable fluorometer (PAM-2500, Walz, Germany). The minimal chlorophyll fluorescence yield (Fo) when all the PSII reaction centers were open was determined via modulated light that was low enough not to induce any significant variable fluorescence (Fv). The maximal chlorophyll fluorescence yield (Fm) when all the reaction centers were closed was determined via a 0.8-s saturating light pulse (7000 μmol · m^{-2} · s^{-1}) on the leaves adapted to darkness for 20 min. The maximal photochemical efficiency was calculated as Fv/Fm = (Fm–Fo)/Fm.

2.8. Measurement of relative electrical conductivity

Membrane damage was assessed by measuring the relative electrical conductivity (REC) of the leaves from the one-month-old plants that were treated at −1 °C or 37 °C in dim light for 24 h immediately before leaf sampling. The leaves from the plants cultured under normal conditions (22 °C) were used as a control. The leaf samples (0.5 g) were cut into small discs and placed in test tubes that contained 10 mL of deionized water for 3 h at 25 °C. Following the incubation, the initial electrical conductivities (S1s) of the solutions were measured with a conductivity meter. The tubes containing the leaf discs were then boiled for 15 min and cooled to room temperature, after which the final electrical conductivity values (S2s) were measured. The REC for each sample was calculated as (S1/S2) × 100%.

2.9. Detection of cell death and ROS

To check cell death and the amount of H_2O_2 produced in plants, staining with Evans Blue or 3,3′-diaminobenzidine (DAB) was performed (Kim et al., 2003; Romero-Puertas et al., 2004). One-month-old transgenic and WT plants were treated at 4 °C or 37 °C in dim light for 24 h, while control plants were not treated. The rosette leaves were sampled and immersed in 0.1% (w/v) aqueous solution of Evans Blue and 1 mg · mL^{-1} DAB solution in 10 mM phosphate buffer (pH 7.8), respectively, as previously described (Kim et al., 2003; Romero-Puertas et al., 2004). Then, the stained samples were bleached in ethanol bath to remove the chlorophyll and embedded in 10% (v/v) glycerol for photographs to be taken.

2.10. Measurement of malondialdehyde content

Lipid peroxidation (LPO) level can be estimated by measuring the malondialdehyde (MDA) accumulation in plant samples (Gill and Tuteja, 2010). One-month-old plants were treated at 4 °C in dim light for 24 h. The measurement was carried out using spectrophotometry with a detection kit (Keming, Suzhou, China) in accordance with the manufacturer's instruction.

2.11. Statistical analysis

Different data sets collected in all of the above-described experiments were presented as the means ± standard deviations (SDs) of at least three independent replicates per experiment. All the experiments on the transgenic lines used WT Arabidopsis as controls. Approximately 60 seeds, 20 seedlings or 20 plants were used for each line in each experiment. Significant differences between the means of each transgenic line (two lines were used) and WT Arabidopsis (the controls) were assessed by using Student's *t*-test at the $P < 0.05$ and $P < 0.01$ levels.

3. Results

3.1. Isolation and in silico analysis of AmGPAT cDNA

The *AmGPAT* gene encodes a protein of 460 amino acid residues with a predicted molecular mass of 50.97 kDa. The protein contains a G-3-P acyltransferase domain between 96 and 171 amino acids in the N-terminal region and a PlsC acyltransferase domain in its C-terminal part (Lewin et al., 1999; Sun et al., 2015). A chloroplast targeting peptide (cTP) of 51 residues was also predicted at its N-terminal. Multiple sequence alignments of the chloroplast GPATs from different species showed that the N-terminal parts and the regions near the C-termini of

these proteins vary quite a lot, but their central regions are highly conserved. The AmGPAT protein contains four highly conserved motifs, AT-I to AT-IV, that have been previously identified in the C-terminal regions of other GPAT proteins (Fig. S1). AmGPAT also contains the conserved residues such as the histidine/H and aspartic acid/D in AT-I, glycine/G in AT-III, and proline/P in AT-IV, which form a catalytically important site of acyltransferases and hence are implicated in catalysis (Lewin et al., 1999; Sui et al., 2007c). There also exist the conserved residues involved in binding to G-3-P substrate in the AmGPAT protein, such as the phenylalanine/F and arginine/R in AT-II and serine/S in AT-III (Lewin et al., 1999; Sui et al., 2007c) (Fig. S1). Notably, a F (226th) residue adjacent to the AT-I motif and an asparagine/N (264th) residue near the AT-II motif were found only in AmGPAT but not in the other GPATs that have the conserved leucine/L and threonine/T or alanine/A residues at the corresponding sites, respectively (Fig. S1). Both the sites are located in the PlsC acyltransferase domain (Fig. S1).

Phylogenetic analysis using the chloroplast GPATs from 15 species revealed that AmGPAT is most closely related to the four GPATs from leguminous plants, including *Glycine soja*, *Cajanus cajan*, *Vigna radiata* and *Pisum sativum*, followed by those from *Cucumis sativus* and *C. moschata*. The remaining eight GPATs, such as Arabidopsis ATS1, tomato LeGPAT and sunflower (*Helianthus annuus*) HaGPAT, are distantly related to AmGPAT (Fig. 1).

3.2. Expression patterns of AmGPAT in different conditions and various organs

To infer the biological functions of *AmGPAT* in response to stressful environments in *A. mongolicus*, we performed expression analyses of this gene in laboratory-cultured *A. mongolicus* seedlings under different stress treatments. As shown in Fig. 2A, the transcript leave of *AmGPAT* significantly increased after exposure to the cold treatment for 2 to 12 h and peaked at 6 h, at which point the expression level was approximately 4.01-fold that of its control (0 h). When the cold treatment lasted for 24 h or 48 h, the transcript level decreased significantly. Throughout the heat treatment, however, the transcript levels significantly decreased to between 0.04- and 0.70-fold that of the control (0 h) (Fig. 2A). Following exposure to 350 mM salt treatment for 2 h and 6 h, the transcript levels significantly declined and then recovered by 12 h and reached 1.60- and 1.31-fold that of the control (0 h) after 24 h and 48 h, respectively (Fig. 2A). By comparison, the transcript levels were 1.20-, 0.91- and 0.53-fold that of the control (0 mM NaCl) after a two-week exposure to 100, 200 and 300 mM NaCl, respectively (Fig. S2). During the drought treatment, compared with the control (0 d) transcript level, the transcript levels increased to between 2.16- and 3.42-fold after 4 to 10 d in the absence of watering but then decreased significantly after 11 d (Fig. 2B).

To obtain more physiologically relevant information about *AmGPAT* in response to abiotic stressors, we then detected its transcription pattern in leaves of *A. mongolicus* shrubs growing in natural field conditions across four different seasons in a full year. As shown in Fig. 2C, the monthly transcript levels of *AmGPAT* were lowest in early August (used as the control), when temperatures were highest during the year [the day/night air temperatures (D/NATs) were approximately 33/20 °C], and highest in early November (9.70-fold that in early August), when the D/NATs were approximately 10/−1 °C. Notably, the transcript levels from early May to early September, when the D/NATs were approximately 19/5 °C to 31/17 °C, were largely lower than those from early October to early April of the following year, when the D/NATs were between approximately 17/5 °C (early October) and −5/−16 °C (early February). With respect to the comparisons among different seasons, the transcript levels were lowest in the summer (average of 1.05-fold that in early August) and highest during the late autumn and winter months (from November to February of the next year; average of 7.64-fold that in early August). The transcript levels of *AmGPAT* were negatively correlated with the ambient temperatures throughout the year. In addition, *AmGPAT* was weakly expressed in the roots (used as the control), twigs and flower buds of *A. mongolicus* shrubs growing in the wild. As expected, the gene was most abundantly expressed in the leaves (43.15-fold that in roots), followed by immature pods (Fig. 2D).

3.3. Constitutive expression of AmGPAT increased the unsaturation of PG and other chloroplast lipids in transgenic Arabidopsis

To characterize the biological functions of *AmGPAT* in plants, we generated transgenic Arabidopsis lines that constitutively express the *AmGPAT* cDNA. After PPT screening, PCR confirmation and semi-quantitative RT-PCR detection (Fig. S3), two transgenic lines (G-1 and G-6) presenting relatively high transcript levels of *AmGPAT* were used for further analyses.

Because of the biochemical importance of chloroplast GPAT in both glycerolipid synthesis and PG unsaturation in chloroplast, we compared the lipids from the leaves of transgenic plants with those from WT leaves. No evident changes in the percentages of MGDG, DGDG, SQDG and PG, four major lipid classes in chloroplast, were detected. However, the fatty acid composition varied, with universal increases in the 18:3 and DBI/UFA levels in each lipid class, especially in PG. The average levels of 18:3 and UFAs (only 18-C UFAs) in PG respectively increased by 17.69% and 19.14%; the increased ratios in the other three lipid classes were 2.43 to 5.11% and 1.05 to 3.65%, respectively. The levels of stearic acid (18:0), 18:1 and 18:2 in PG also increased markedly, which was accompanied by the decreases in the 16:0 and 16:1*t* levels. The 16:0 levels in MGDG and DGDG also decreased greatly. Moreover, the hexadecadienoic acid (16:2) level in MGDG and both 16:2 and hexadecatrienoic acid (16:3) levels in DGDG increased markedly (Table 1). Together, these results indicate that constitutive expression of *AmGPAT* increased the unsaturation of all the measured glycerolipids in chloroplast membranes, especially that of PG, primarily through raising the levels of 18:3.

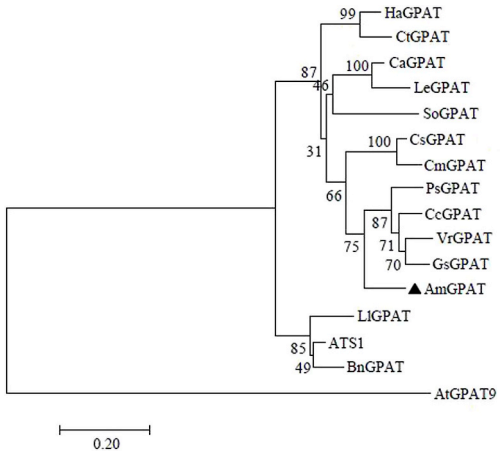

Fig. 1. Phylogenetic tree of AmGPAT and other chloroplast GPATs from different plant species. The accession number for each GPAT sequence in GenBank is as follows: *A. mongolicus* AmGPAT, MK482343; *A. thaliana* ATS1, OAP16056.1; *Brassica napus* BnGPAT, XP_013677342; *C.annuum* CaGPAT, AAP79443.2; *C. cajan* CcGPAT, XP_020216491.1; *C. moschata* CmGPAT, BAB17755; *C. sativus* CsGPAT, NP_001292631; *Carthamus tinctorius* CtGPAT, AAA74319.1; *G. soja* GsGPAT, KHN38956.1; *H. annuus* HaGPAT, ADV16382; *L. esculentum* LeGPAT, ABE28022.1; *Lepidium latifolium* LlGPAT, AEU10135.1; *P. sativum* PsGPAT, CAA41769.1; *S. oleracea* SoGPAT, XP_021852023; and *V. radiata* VrGPAT, XP_014521075.1. The phylogenetic tree was inferred using the NJ method in MEGA 7.0 software. The number at each node represents the bootstrap percentage. Arabidopsis endoplasmic reticulum-localized AtGPAT9 (ACT32031.1) was used as an outgroup.

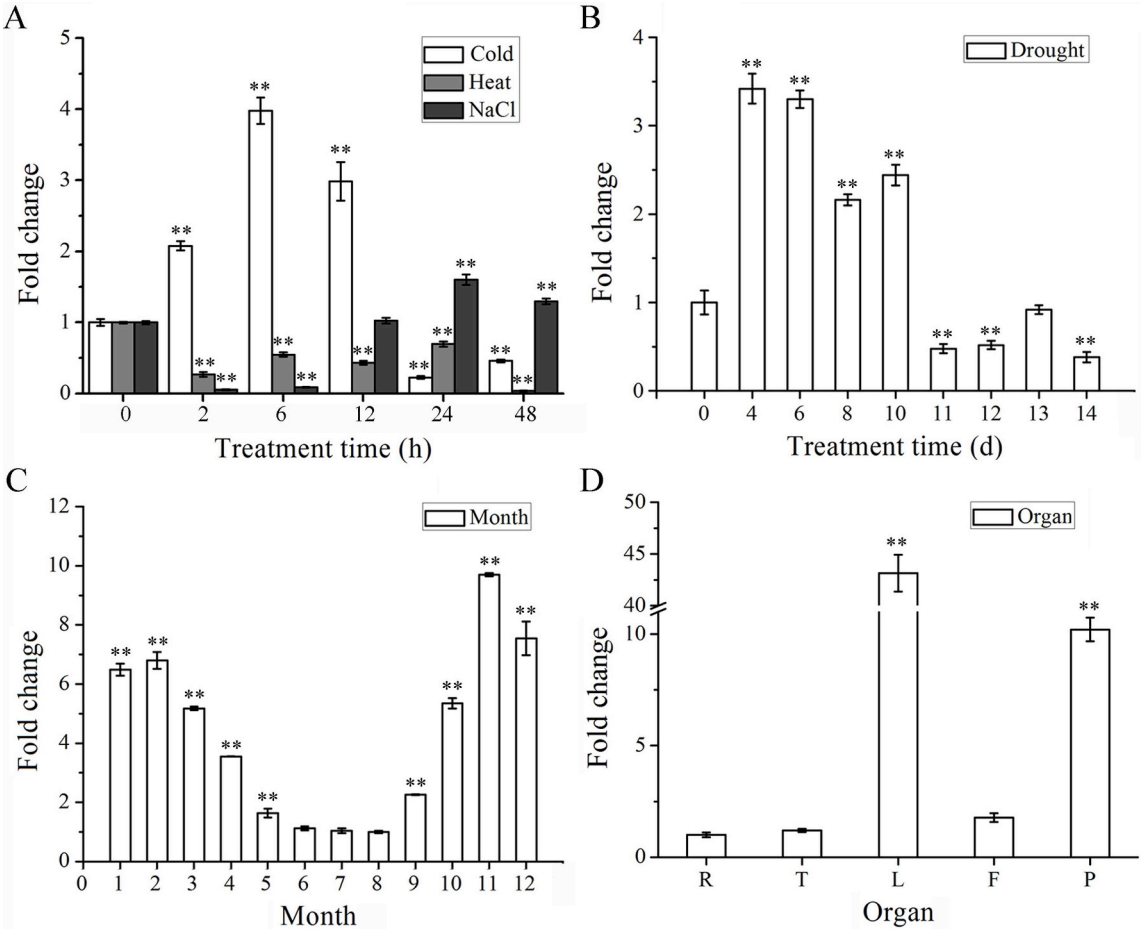

Fig. 2. Expression patterns of *AmGPAT* in different stress conditions, different seasons and different organs.
A, The expression patterns in *A. mongolicus* seedlings under the cold (4 °C to −6 °C), heat (42 °C) and salt (350 mM NaCl) treatments. B, The expression pattern in *A. mongolicus* seedlings under the drought (stop watering) treatment. C, The expression pattern in monthly sampled young leaves of *A. mongolicus* shrubs in a full year. D, The expression pattern in different organs (R, roots; T, twigs; L, leaves; F, flower buds; P, immature pods). The expression values at 0 h and 0 d, as well as in early August and in the roots (both had the lowest expression levels), were normalized to 1.0 for the expression assays. Bars indicate SDs (n = 3), and asterisks indicate significant differences between each stress treatment, each month or each organ and its control at $P < 0.01$.

3.4. Constitutive expression of AmGPAT increased the tolerance to chilling and freezing but reduced heat tolerance of transgenic Arabidopsis

3.4.1. Increased chilling tolerance

When cultured under normal growth conditions, the transgenic and WT plants displayed no clear difference in appearance during their entire life cycles (data not shown). Moreover, no obvious difference in seedling growth between the two sets of plants was observed during their incubation at 8 °C in dim light for two weeks (Fig. 3B). However, after returning to normal growth conditions for recovery, the growth of the transgenic seedlings was better than that of the WT seedlings (Fig. 3C, D and E). After two weeks of recovery growth, the fresh weights of the aerial parts of the G-1 and G-6 plants were 144.62 ± 10.44 and 135.13 ± 8.52 mg·plant^{-1}, respectively, while that of the WT plants was 110.21 ± 7.34 mg·plant^{-1} (Fig. 3D); the heights of the G-1 and G-6 plants were 7.32 ± 1.31 and 4.71 ± 0.73 cm, respectively, while that of the WT plants was 3.80 ± 1.14 cm (Fig. 3E).

The maximal photochemical efficiency of PSII (Fv/Fm) value is an important indicator of the photoinhibition of PSII under stress conditions. Under normal growth conditions, both transgenic and WT plants had Fv/Fm values close to 0.80. After exposure to chilling treatment for 5 h and 10 h in high light, the values in all of the plants dropped markedly, with a slightly lesser decrease in two transgenic lines compared to the WT plants. At the end of the chilling treatment, the Fv/Fm values of the G-1, G-6 and WT plants decreased by 54.90%, 59.67% and 69.41% compared with their initial values, respectively. However, after returning to normal growth conditions, the transgenic plants displayed a clearly more rapid recovery in the Fv/Fm values compared to the WT plants. At 18 h of the recovery period, the G-1 and G-6 plants recovered their Fv/Fm to an average level of 94.81% of their initial values before the chilling treatment. In contrast, the WT plants recovered their Fv/Fm to the level of 76.79% (Fig. 3F).

We also detected cell death in the leaves of the chilling-treated plants (4 °C for 24 h in dim light) using Evans blue staining. Compared to WT plants, the transgenic lines, especially G-1, displayed fewer dark blue patches on the leaves (Fig. 3G), indicating that the transgenics had decreased cell death under the chilling stress.

Collectively, these data indicate that constitutive expression of *AmGPAT* markedly accelerated the recovery of the transgenic plants from both growth suppression and PSII photoinhibition and reduced the cell death induced by the chilling treatments.

3.4.2. Increased freezing tolerance

When treated at −6 °C for 8 h after a pretreatment at 4 °C for 24 h and a post-treatment at 4 °C for 12 h again, almost all of the WT seedlings were severely damaged and died; the surviving seedlings resumed growth slowly during the subsequent recovery period under normal growth conditions. In contrast, only some of the transgenic seedlings exhibited severe damage and died; most of the surviving seedlings

Table 1
Fatty acid composition of chloroplast lipids isolated from the leaves of transgenic and wild type Arabidopsis plants.

Lipid class	Genotype	Percentage of total lipids	Fatty acid composition (mol%)								
			16:0	16:1[a]	16:2	16:3	18:0	18:1	18:2	18:3	DBI
MGDG	WT	57.85	1.85	0.36	1.88	34.92	0.23	0.68	2.45	57.63	287.35
	G-1	57.79	1.17** (−36.76)[b]	0.14** (−61.11)	2.16* (14.89)	34.82 (−0.29)	0.20 (−13.04)	0.52* (−23.53)	2.06 (−15.92)	58.93 (2.26)	290.35 (1.04)
	G-6	57.89	1.18** (−36.22) [-36.49][c]	0.12** (−66.67) [-63.89]	2.15* (14.36) [14.63]	34.65 (−0.77) [-0.53]	0.20 (−13.04) [-13.04]	0.51* (−25.00) [-24.27]	2.06 (−15.92) [-15.92]	59.13 (2.60) [2.43]	290.39 (1.06) [1.05]
DGDG	WT	23.16	15.22	0.12	0.64	1.85	1.61	1.24	5.61	73.71	240.54
	G-1	23.75	13.42* (−11.83)	0.13 (8.33)	0.80* (25.00)	2.93** (58.38)	1.16* (−27.95)	0.81** (−34.68)	4.53* (−19.25)	76.22 (3.41)	249.05 (3.54)
	G-6	23.11	14.06 (−7.62) [-9.73]	0.21** (75.00) [41.67]	0.92** (43.75) [34.38]	3.46** (87.03) [72.71]	0.98** (−39.13) [-33.54]	0.72** (−41.94) [-38.31]	4.48* (−20.14) [-19.70]	75.17 (1.98) [2.70]	247.62 (2.94) [3.24]
PG	WT	14.52	32.64	21.65	-[d]	–	1.31	5.06	8.62	30.72	114.46
	G-1	13.94	23.32** (−28.55)	18.20* (−15.94)	–	–	2.97** (126.72)	7.94** (56.92)	10.23* (18.68)	37.34** (21.55)	140.42** (22.68)
	G-6	14.45	26.70** (−18.20) [-23.38]	17.93* (−17.18) [-16.56]	–	–	2.84** (116.79) [121.76]	7.72** (52.57) [54.75]	9.84 (14.15) [16.42]	34.97** (13.83) [17.69]	132.31** (15.59) [19.14]
SQDG	WT	4.47	44.08	–	–	–	6.11	3.56	7.53	38.72	134.78
	G-1	4.52	43.75 (−0.75)	–	–	–	5.07 (−17.02)	3.27 (−8.15)	6.95 (−7.70)	40.96 (5.79)	140.05 (3.91)
	G-6	4.55	43.31 (−1.75) [-1.25]	–	–	–	5.77 (−5.56) [-11.29]	2.94 (−17.42) [-12.79]	7.55 (0.27) [-3.72]	40.43 (4.42) [5.11]	139.33 (3.38) [3.65]

DBI is the sum of the *cis*-UFA levels.

[a] The 16:1 represents 16:1*t* in PG.

[b] The numbers in each parentheses represent the changed ratios for the transgenic lines (G-1 and G-6) compared to WT plants.

[c] The numbers in each square brackets represent the averages of changed ratios in two transgenic lines compared to WT plants.

[d] The dashes represent < 0.1 mol%. The values are the means of the results obtained from three independent experiments. The asterisks indicate significant differences of the transgenic lines compared to WT (*, $P < 0.05$; **, $P < 0.01$).

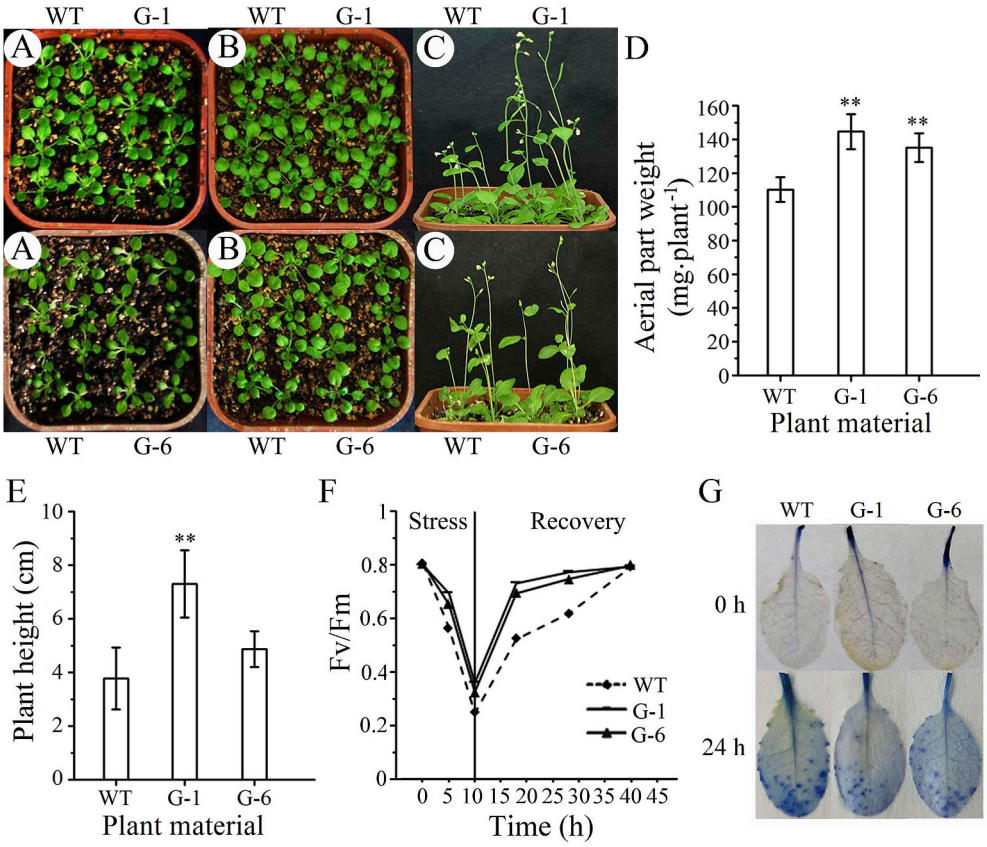

Fig. 3. Constitutive expression of *AmGPAT* enhanced chilling tolerance of transgenic Arabidopsis.
A, Two-week-old seedlings before the chilling treatment. B, Seedlings after two weeks of the chilling treatment (8 °C in dim light). C, Plant phenotypes after two weeks of recovery under normal growth conditions. D and E, Fresh weights of aerial parts and plant heights after two weeks of recovery growth. F, Fv/Fm during the chilling treatment (6 °C for 10 h under a light level of 600 μmol·m^{-2}·s^{-1}) and subsequent recovery. G, Cell death detected by Evans blue staining of the leaves from the plants treated at 4 °C for 24 h. WT represents wild type; G-1 and G-6 represent two independent transgenic lines. Bars indicate SDs (n = 3), and asterisks indicate significant differences of transgenic lines compared to WT (**, P < 0.01). (For interpretation of the references to color in this figure legend, the reader is referred to the Web version of this article.)

continued to grow quite rapidly during recovery (Fig. 4B, C, D, E and F). After two weeks of recovery, survival rates of the WT, G-1 and G-6 seedlings were 45.33 ± 7.84%, 83.32 ± 9.43% and 65.21 ± 8.13%, respectively (Fig. 4E). After an additional two weeks of recovery, the transgenic lines had average plant heights of 5.74 ± 0.82 (G-1) and 4.81 ± 1.22 cm (G-6), while that of the WT plants was 2.74 ± 0.93 cm (Fig. 4F). These results indicate that constitutive expression of *AmGPAT* significantly enhanced the survival and regrowth capacity of transgenic lines under the freezing treatment.

Relative electrical conductivity is mainly used to reflect the damage of cellular membranes. When cultured under 22 °C, the transgenic and WT plants presented similar REC values. However, after exposure to −1 °C for 24 h, the REC values of the G-1 and G-6 plants increased to 35.34 ± 1.64% and 39.91 ± 2.28%, respectively, which were significantly lower than the value (48.53 ± 0.89%) of the WT plants (Fig. 4G). Thus, constitutive expression of *AmGPAT* reduced cell membrane damage under the freezing treatment.

3.4.3. Reduced heat tolerance

We also performed heat tolerance assays at 54 °C for 2 h after a pretreatment at 37 °C for 2 h and at 22 °C for an additional 2 h. At the end of the treatment, clear withering appeared at the leaf tips or leaf edges of the transgenic seedlings, whereas only slight withering was observed at some leaf tips of the WT seedlings. During subsequent recovery under normal growth conditions, the transgenics showed poor performance in both growth and development compared to their WT counterparts (Fig. 5B, C, D, E and F). After four weeks of recovery, the fresh weights of aerial parts of the G-1 and G-6 plants were 155.83 ± 11.72 and 164.62 ± 7.44 mg·plant^{-1}, respectively, while that of the WT plants was 217.37 ± 12.78 mg·plant^{-1} (Fig. 5E). Furthermore, the fresh silique weights of the G-1 and G-6 plants were respectively 6.42 ± 0.64 and 8.71 ± 1.23 mg·plant^{-1}, whereas that of the WT plants was 17.92 ± 1.64 mg·plant^{-1} (Fig. 5F). After exposure to 37 °C for 24 h, the REC values of the leaves from the transgenics were 42.09 ± 2.32% (G-1) and 40.52 ± 0.84% (G-6), while that of the WT leaves was 33.31 ± 1.24% (Fig. 5G). The assays using Evans blue staining showed increased cell death in the transgenic plants compared with the WT plants under the heat treatment (Fig. 5H). Therefore, constitutive expression of *AmGPAT* reduced heat tolerance of transgenic lines.

We also investigated the effect of *AmGPAT* expression on drought and salt tolerances of the transgenic lines at different stages during their entire life cycles, but no significant effects were observed under our experimental conditions (data not shown).

3.5. Constitutive expression of AmGPAT increased the tolerance of transgenic Arabidopsis to oxidative stress

To investigate whether *AmGPAT* affects tolerance to oxidative stress, we first detected the accumulation of H_2O_2, an important ROS species, in the chilling-treated leaves using DAB staining. The brown-color patches were relatively sparser in the transgenics than in the WT leaves, indicating that transgenic plants accumulated less H_2O_2 than WT plants under the chilling treatment (Fig. 6A). We next measured the contents of MDA, an important indicator of LPO in membranes (Gill and Tuteja, 2010), in leaves of the transgenic and WT plants under chilling stress. Under normal growth conditions, the MDA contents in G-1 and G-6 lines were slightly lower than that in WT leaves. After exposure to 4 °C for 24 h, the MDA contents increased clearly in all of the plants, but the increase was significantly lesser in the G-1and G-6 plants than in the WT plants (Fig. 6B).

We also tested the tolerance to exogenous H_2O_2 at the seed germination stage. Consistent with the MDA data, both G-1 and G-6 lines germinated quicker and grew better than did the WT controls on the media containing different concentrations of H_2O_2 (Fig. 6D, E, F and G). For instance, after germinating on the medium with 4 mM H_2O_2 for 8 d, 68.34 ± 7.62% and 63.28 ± 2.83% of the G-1 and G-6 lines' seeds germinated (emergence of green cotyledons), respectively, but only

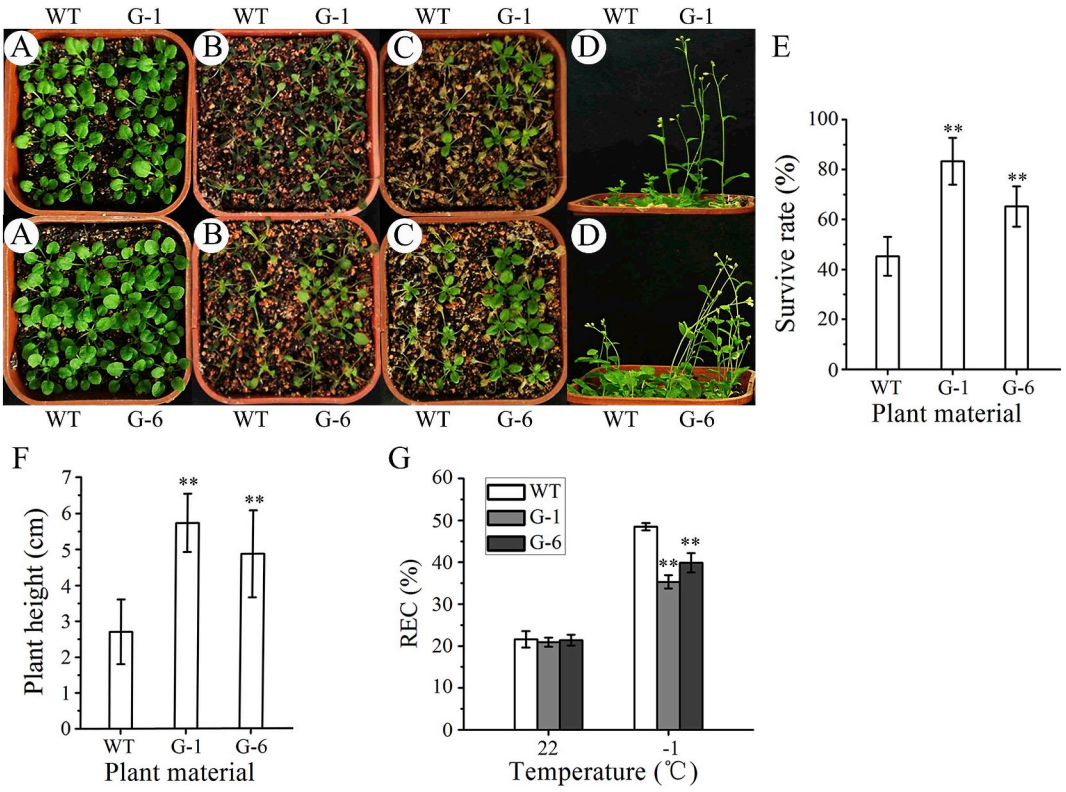

Fig. 4. Constitutive expression of *AmGPAT* enhanced freezing tolerance of transgenic Arabidopsis.A, Two-week old seedlings before the freezing treatment. B, C and D, The phenotypes of the freezing-treated seedlings after 3, 12 and 28 d of recovery under normal growth conditions, respectively. E and F, Survival rates and plant heights after two weeks and four weeks of recovery, respectively. G, REC of the leaves from the plants treated at −1 °C for 24 h. WT represents wild type; G-1 and G-6 represent two independent transgenic lines. Bars indicate SDs (n = 3), and asterisks indicate significant differences of the transgenic lines compared to WT (**, $P < 0.01$).

31.64 ± 7.61% of the WT seeds germinated. At the same time point, the fresh weights of the transgenic seedlings growing on the same medium reached 34.05 ± 2.92 (G-1) and 30.43 ± 2.51 mg (G-6) per 20 seedlings, while the WT seedlings had a fresh weight of only 9.43 ± 1.32 mg (Fig. 6 F and G). On 1/2 MS medium (no stress), both seed germination and seedling growth showed no discernable difference between the transgenic lines and their WT control (Fig. 6C).

Together, these assays demonstrated that the introduction of *AmGPAT* improved the tolerance of the transgenic lines to chilling-induced oxidative damage and the exogenous H_2O_2 stressor.

4. Discussion

In spite of the extensive studies and remarkable progress in *GPATs* from several species, studies on these genes in woody plants with strong tolerance to abiotic stressors have not been reported. In this study, we isolated and functionally characterized *AmGPAT* from *A. mongolicus*, a desert shrub with very high tolerance to extremely low temperatures during severe winters. The AmGPAT sequence contains all essential domains, conserved motifs and the targeting peptide to chloroplast as well as the conserved residues existing in its homologous proteins from other plant species. Interestingly, AmGPAT also contains two unique residues in its key central region compared to other GPATs: one is the 226F residue adjacent to the AT-I motif, and another is the 264N near the AT-II motif (Fig. S1). Both the unique residues are located in the PlsC acyltransferase domain (Lewin et al., 1999; Sun et al., 2015) and hence may affect the enzyme's activity. Moreover, the AmGPAT sequence shares high homology with the chloroplast GPATs from other leguminous plants (Fig. 1). These features indicate that *AmGPAT* encodes a canonical chloroplast GPAT that should have the capacity to initiate the syntheses of chloroplast membrane lipids such as PG. Our functional analyses of this gene at the expression and stress tolerance levels in this work provide further evidence for this inference.

4.1. AmGPAT may play important roles in the response and endurance of A. mongolicus to harsh desert climate

Expression analysis of genes in response to abiotic stressors can provide important information about their function in stress tolerance in plants. However, compared to the researches on their biochemical and stress-tolerant functions, attention to the expression pattern of *GPATs* has been limited, as described in the introduction of this paper. Here, we detected that the transcription of *AmGPAT* was rapidly induced by the cold treatment but significantly inhibited during the heat exposure in laboratory-cultured *A. mongolicus* seedlings (Fig. 2A). More importantly, a negative correlation between the transcript levels of *AmGPAT* in the leaves of the wild-growing *A. mongolicus* shrubs and the ambient temperatures was found during a full year of our sampling (Fig. 2C). Consistent with these observations, the transgenic lines showed an increase in both chilling and freezing tolerances but a decrease in heat tolerance (Figs. 3–5). These results suggest that *AmGPAT* might have acquired the capacity to acclimate to the seasonally low or high temperatures in the wild by altering its expression; that is to say, during the chilling and freezing months, the gene was abundantly expressed to provide a high degree of unsaturation of PG and probably other chloroplast lipids and hence the fluidity and integrity of the chloroplast membranes, sustaining the membrane performance under the chilling and freezing weather. In contrast, a low expression of this gene during the warm and hot months might be beneficial to maintain the membrane saturation and stability and thus enhance the tolerance

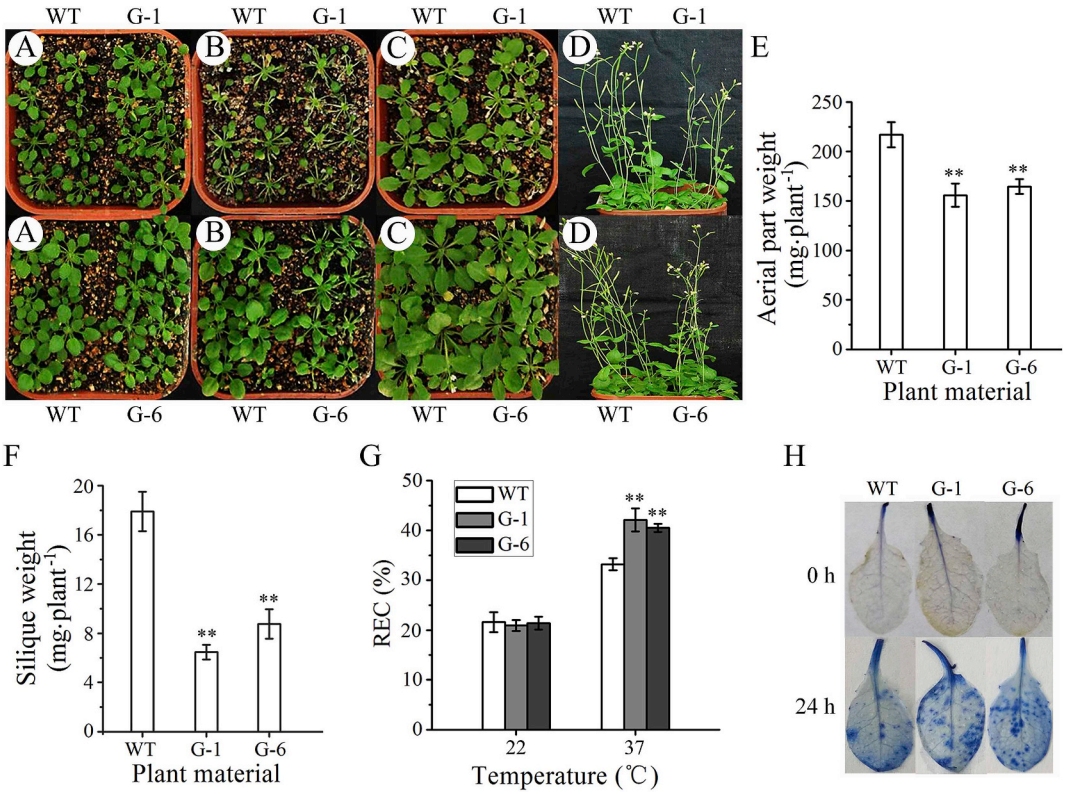

Fig. 5. Constitutive expression of *AmGPAT* reduced heat tolerance of transgenic Arabidopsis.A, Eighteen-day-old seedlings before the heat treatment. B, C and D, The phenotypes of the heat-treated seedlings after 3, 12 and 28 d of recovery under normal growth conditions, respectively. E and F, Fresh weights of aerial parts and siliques after four weeks of recovery, respectively. G, REC of the leaves from the plants exposed to 37 ˚C for 24 h. H, Cell death detected by Evans blue staining of the leaves from the plants treated at 37 ˚C for 24 h. WT represents wild type; G-1 and G-6 represent two independent transgenic lines. Bars indicate SDs (n = 3), and asterisks indicate significant differences of the transgenic lines compared to WT (**, P < 0.01) . (For interpretation of the references to color in this figure legend, the reader is referred to the Web version of this article.)

against the desert heat. Interestingly, *LeGPAT* in chilling-sensitive tomato also showed a similar dual performance in response and tolerance to chilling and elevated temperatures, and the tolerance performance was likely due to the LeGPAT enzyme's selectivity for 18:1 over 16:0 (Sui et al., 2007a, 2007b, 2007c; Sun et al., 2011). Moreover, the transcription of *AmGPAT* was rapidly and lastingly induced by the drought treatment (Fig. 2B), suggesting its possible involvement in the endurance of *A. mongolicus* to arid desert climate, although no visible changes were observed in the transgenics in our drought tolerance assays.

4.2. AmGPAT may affect stress tolerance by changing the unsaturation of other chloroplast lipids except for PG

Previous studies have shown that chloroplast GPATs from different plants affect the tolerance to low or high temperature and high salinity through controlling the fatty acid composition at the *sn*-1 position of PG in thylakoid membranes (Murata et al., 1992; Moon et al., 1995; Yokoi et al., 1998; Ariizumi et al., 2002; Sakamoto et al., 2003; Sui et al., 2007a, 2007c, 2017; Sun et al., 2010; Sun et al., 2011; Ivanov et al., 2012). The GPATs from cold-tolerant plants displayed a substrate preference for 18:1 vs. 16:0 and eventually enhanced chilling tolerance through increasing the relative level of 18-C UFAs in PG (Murata et al., 1992; Yokoi et al., 1998; Ariizumi et al., 2002). Our current data (Table 1, Fig. 3) are consistent with these reports. Moreover, our study showed slight increases in the unsaturation of MGDG, DGDG and SQDG in the transgenic plants primarily through raising the levels of 18:3 (Table 1). Opposite changes have been previously found in transgenic tobacco with *CmGPAT* from the cold-sensitive plant squash, in which the unsaturation of MGDG, DGDG, SQDG and PG, particularly that of PG, decreased mainly through the reduction in the 18:3 levels. Correspondingly, the chilling tolerance of the photosynthetic machinery declined (Moon et al., 1995). Therefore, it seems likely that chloroplast GPAT could also affect the fatty acid composition at the *sn*-1 position of other chloroplast lipids, except for PG. In this study, the substantially increased UFAs, particularly 18:3, in PG might play an important role in protecting the thylakoid membranes against stress injury, while those in other lipids, despite their small increases, might be helpful to the structure and function of the chloroplast membrane systems under certain abiotic stresses.

4.3. AmGPAT may play a crucial role in both chilling and freezing tolerances

Chilling temperatures can reduce the fluidity and integrity of chloroplast membranes and, ultimately, inhibits the activity of the photosynthetic apparatus (Wada and Murata, 2007; Los et al., 2013). The photoinhibition of PSII in thylakoid membranes is a well-known chilling injury to chloroplast and is considered the major cause of photosynthesis reduction of plants under chilling conditions. The entire course of the photoinhibition includes the inactivation process and the recovery process, and chilling stress has been found to act primarily to inhibit the latter process (Nishiyama and Murata, 2014). The PG molecules are particularly enriched in PSII (Sheng et al., 2018). Previous studies on the *GPATs* from squash and tomato have revealed that the unsaturated PGs play a crucial role in promoting the recovery of the chilling-induced photoinhibition of PSII (Moon et al., 1995; Sun et al., 2011). Consistent with these findings, our current data showed that the

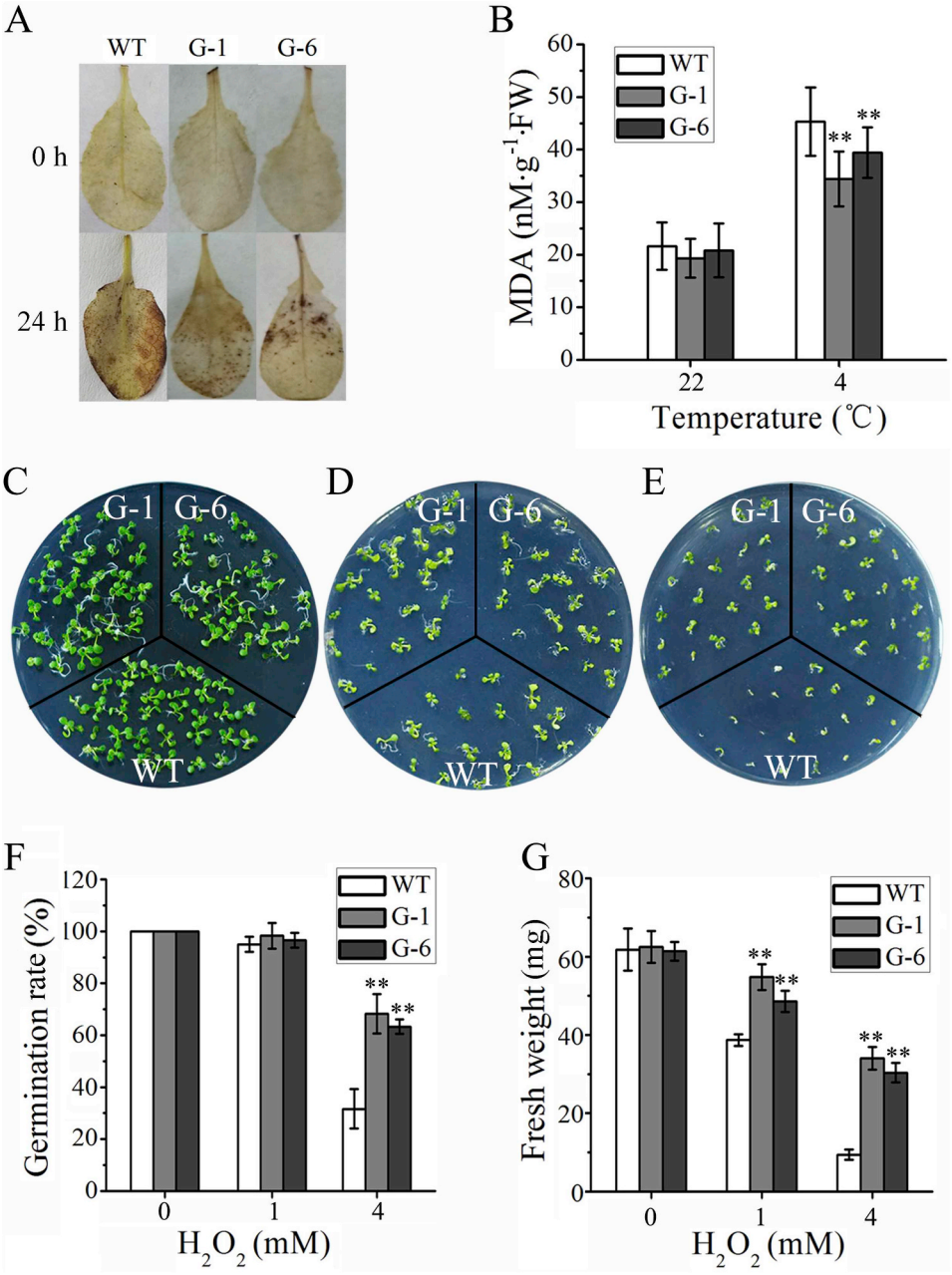

Fig. 6. Constitutive expression of *AmGPAT* enhanced oxidative stress tolerance of transgenic Arabidopsis. A and B, The DAB staining of and MDA contents in the leaves of the plants exposed to 4 °C for 24 h (0 h or 22 °C as the control). C, D and E, Seed germination and subsequent growth on 1/2 MS media containing 0 (control), 1 and 4 mM H_2O_2, respectively. Images were taken at 8 d of the germination period. F and G, Germination rates and fresh weights (mg per 20 seedlings) after 8 d on 1/2 MS media containing different concentrations of H_2O_2. WT represents wild type; G-1 and G-6 represent two independent transgenic lines. Bars indicate SDs (n = 3), and asterisks indicate significant differences of the transgenic lines compared to WT (**, P < 0.01).

increased change in the PG unsaturation primarily accelerated the recovery of transgenic plants from the photoinhibition of PSII and the growth suppression after the chilling treatment (Fig. 3). D1 protein is an essential component in the PSII reaction center, and its turnover is a determining event for the repair of the inactivated PSII (Nishiyama and Murata, 2014). Phosphatidylglycerol was found to specially interact with D1 (Wada and Murata, 2007). Thus, the increased UFA level of PG (Table 1) could probably provide a flexible membrane surrounding for the turnover of Dl protein, thereby promoting the recovery of the PSII complex and, futher, the growth of transgenic seedlings during the post-chilling period (Fig. 3) (Wada and Murata, 2007; Nishiyama and Murata, 2014). The increased unsaturation of other thylakoid lipids such as DGDG and SQDG (Table 1) might also contribute to the recovery.

Compared with chilling, freezing temperatures can cause more severe damage to cellular membranes and even lead to cell death. The freezing-caused membrane damage occurs in different forms, such as lamellar-to-hexagonal-II (H_{II}) phase transition and the membrane rupture of chloroplasts (Moellering et al., 2010). It has long been recognized that increased changes in fatty acid unsaturation and lipid content of membranes during cold acclimation play important roles in plants against freezing damage (Heidarvand and Amiri, 2010; Moellering et al., 2010; Los et al., 2013). However, whether chloroplast GPAT affects freezing tolerance of plants has not been documented. In this study, we found that the increase in chloroplast lipid (mainly PG) unsaturation obviously improved the freezing tolerance of transgenic plants (Fig. 4). *Ammopiptanthus mongolicus* is a relic shrub in the cold-temperate desert (Wu et al., 2014; Yin et al., 2018). We thus speculate that *AmGPAT* might have acquired specific functions during evolution of the species and may play a crucial role for the survival of *A. mongolicus* plants in the wild during severe winters, likely through similar mechanisms to those found in the transgenic plants. Recent studies on Arabidopsis revealed that the conversion from MGDG to DGDG and oligogalactolipids that are not prone to form non-bilayer H_{II} phase at the outer chloroplast envelope membrane is critical for freezing tolerance (Moellering et al., 2010; Los et al., 2013). The reaction is catalyzed

by the galactolipid: galactolipid galactosyltransferase (GGGT) localized in the outer chloroplast membrane (Moellering et al., 2010). The increased UFAs in *AmGPAT* transgenic plants might help to maintain or recover the activities of membrane proteins such as GGGT and hence may function in preventing chloroplast rupture by inhibiting the formation of non-bilayer H_{II}-type structures after freezing (Moellering et al., 2010; Los et al., 2013). However, all these possibilities need to be experimentally tested further.

4.4. AmGPAT may closely correlate with the tolerance to oxidative stress

Reactive oxygen species comprise both free radicals such as superoxide radicals ($O_2^{\cdot-}$) and non-radical (molecular) forms such as H_2O_2 (Gill and Tuteja, 2010). Overproduction of ROS is a common phenomenon occurring in plant cells under various abiotic stresses and results in secondary oxidative stress that, coupled with other deleterious effects of abiotic stress, ultimately lead to severe cell injury or cell death (Gill and Tuteja, 2010; Nishiyama and Murata, 2014). H_2O_2 is a moderately reactive and toxic but relatively more stable and more diffusive ROS. Excessive H_2O_2 can cause damage to plant cells, such as inactivating enzymes, causing LPO, and leading to cell death (Gill and Tuteja, 2010). Our current study demonstrated that *AmGPAT* played important roles in reducing the chilling-induced overproduction of H_2O_2 and the exogenous H_2O_2-exerted suppression in seed germination and subsequent seedling growth (Fig. 6). We speculate that the increased unsaturation of the chloroplast lipids may help to increase the activities of the antioxidant enzymes in chloroplast and thus improve the capacity to scavenge excessive H_2O_2 in the transgenic plants. Relevant evidence has been found in a previous study on tomato *LeGPAT* that increased the activities of superoxide dismutase and ascorbate peroxidase, two antioxidant enzymes, and reduced the contents of $O_2^{\cdot-}$ and H_2O_2 under chilling stress (Sui et al., 2007a; Sun et al., 2011).

Lipid peroxidation is considered the most damaging process known to occur in every living organism, especially in thylakoid membranes in chloroplast because of their abundance in UFAs (Gill and Tuteja, 2010). In addition to the direct harmful effect of LPO on normal cellular functioning, the products of LPO, such as MDA and 4-hydroxy-2-nonenal, can also cause damages to plant cells, such as decreasing membrane fluidity, increasing membrane leakage and inactivating membrane proteins, by reacting with macromolecules (Gill and Tuteja, 2010). Here, we found that constitutive expression of *AmGPAT* in Arabidopsis caused a significant decrease in the MDA content in transgenic lines (Fig. 6B), indicating an important role of *AmGPAT* in the alleviation of chilling-induced LPO. This finding is consistent with earlier observations in the H_2O_2 assays (Fig. 6A, D, E, F and G). It seems that the increased UFAs through the expression of *AmGPAT* may be conducive to improving the membrane fluidity and integrity and thus the activities of antioxidant enzymes in chloroplast, leading to the inhibition of LPO in the chloroplast membranes.

Collectively, our current results indicate that AmGPAT played an important role in tolerating oxidative stress, likely through increasing the unsaturation of chloroplast lipids, which in turn may reduce the chilling injury to chloroplasts and cells.

5. Conclusions

This study is the first to identify a chloroplast GPAT gene (named *AmGPAT*) from *A. mongolicus*, an evergreen broadleaf shrub distributed in the central Asian desert. The transcript levels of *AmGPAT* showed an obvious negative correlation with the stress temperatures imposed in both the laboratory and the natural habitat. Overall, the transcription was also induced by drought but inhibited by high salinity. Constitutive expression of *AmGPAT* in Arabidopsis increased the UFA levels mainly in PG but also in other chloroplast lipids and thus enhanced chilling tolerance but reduced heat tolerance of the transgenic plants such as did the *GPATs* from other species. Interestingly, the *AmGPAT* expression also significantly enhanced the tolerance to freezing and oxidative stress, likely through increasing the unsaturation of the lipids in chloroplast membranes. These findings improve the current understanding of the role of chloroplast GPAT in plant tolerance to abiotic stressors by regulating the unsaturation of chloroplast lipids. We suggest that an increase in UFAs, especially in 18:3, in chloroplast lipids might be crucial to maintaining membrane fluidity, integrity and functioning under chilling, freezing and oxidative stress. In-depth investigations on these aspects in both transgenic plants and *A. mongolicus* are needed in the future.

Contributions

Min Xue and Ting Guo performed the experiments, analyzed and interpreted the data, and prepared the figures with assistance from Meiyan Ren, Kuangang Tang and Wenjun Zhang. Min Xue also drafted, edited and submitted the manuscript with assistance from Meiyan Ren. Maoyan Wang designed and supervised the experiments and revised the manuscript. Zhilin Wang contributed to the design and guidance of the experiments. All authors discussed the results and approved the final manuscript.

Conflicts of interest

The authors declare that they have no conflict of interests.

Acknowledgements

This work was funded by the Major Project of Natural Science Fund of Inner Mongolia Autonomous Region (grant number 2012ZD02), the National Natural Science Foundation of China (grant numbers 30960158 and 31260256), and the Science and Technology Innovative Group Fund of Inner Mongolia Autonomous Region (grant number 201503004). The authors would like to thank Prof. Yinong Xu (Laboratory of Photosynthesis and Environmental Molecular Physiology, Institute of Botany, Chinese Academy of Sciences) for his help in the design of the study and the preparation of this manuscript and Prof. Fuying Feng (College of Life Sciences, Inner Mongolia Agricultural University) for his help in the lipid analysis.

Appendix A. Supplementary data

Supplementary data to this article can be found online at https://doi.org/10.1016/j.plaphy.2019.07.019.

References

Ariizumi, T., Kishitani, S., Inatsugi, R., Nishida, I., Murata, N., Toriyama, K., 2002. An increase in unsaturation of fatty acids in phosphatidylglycerol from leaves improves the rates of photosynthesis and growth at low temperatures in transgenic rice seedlings. Plant Cell Physiol. 43 (7), 751–758. https://doi.org/10.1093/pcp/pcf087.

Botella, C., Sautron, E., Boudiere, L., Michaud, M., Dubots, E., Yamaryo-Botté, Y., Albrieux, C., Marechal, E., Block, M.A., Jouhet, J., 2016. ALA10, a phospholipid flippase, controls FAD2/FAD3 desaturtion of phosphatidylcholine in the ER and affects chloroplast lipid composition in *Arabidopsis thaliana*. Plant Physiol. 170 (3), 1300–1314. https://doi.org/10.1104/pp.15.01557.

Chen, X., Snyder, C.L., Truksa, M., Shah, S., Weselake, R.J., 2011. *sn*-Glycerol-3-phosphate acyltransferases in plants. Plant Signal Behav. 6 (11), 1695–1699. https://doi.org/10.4161/psb.6.11.17777.

Gill, S.S., Tuteja, N., 2010. Reactive oxugen species and antioxidant machinery in abiotic stress tolerance in crop plants. Plant Physiol. Biochem. 48 (12), 909–930. https://doi.org/10.1016/j.plaphy.2010.08.016.

Gupta, S.M., Pandey, P., Grover, A., Patade, V.Y., Singh, S., Ahmed, Z., 2013. Cloning and characterization of GPAT gene from *Lepidium latifolium* L.: a step towards translational research in agri-genomics for food and fuel. Mol. Biol. Rep. 40 (7), 4235–4240. https://doi.org/10.1007/s11033-013-2505-7.

Heidarvand, L., Amiri, R.M., 2010. What happens in plant molecular responses to cold stress? Acta Physiol. Plant 32 (3), 419–431. https://doi.org/10.1007/s11738-009-0451-8.

Ivanov, A.G., Allakhverdiev, S.I., Huner, N.P.A., Murata, N., 2012. Genetic decrease in fatty acid unsaturation of phosphatidylglycerol increased photoinhibition of

photosystem I at low temperature in tobacco leaves. Biochim. Biophys. Acta 1817 (8), 1374–1379. https://doi.org/10.1016/j.bbabio.2012.03.010.
Kim, M., Ahn, J.W., Jin, U.H., Choi, D., Paek, K.H., Pai, H.S., 2003. Activation of the programmed cell death pathway by inhibition of proteasome function in plants. J. Biol. Chem. 278 (21), 19406–19415. https://doi.org/10.1074/jbc.M210539200.
Kratsch, H.A., Wise, R.R., 2000. The ultrastructure of chilling stress. Plant Cell Environ. 23, 337–350. https://doi.org/10.1046/j.1365-3040.2000.00560.x.
Lewin, T.M., Wang, P., Coleman, R.A., 1999. Analysis of amino acid motifs diagnostic for the sn-glycerol-3-phosphate acyltransferase reaction. Biochemistry 38 (18), 5764–5771. https://doi.org/10.1021/bi982805d.
Li, X.T., Liu, P., Yang, P.P., Fan, C.Z., Sun, X.M., 2018. Characterization of the glycerol-3-phosphate acyltransferase gene and its real-time expression under cold stress in *Paeonia lactiflora* Pall. PLoS One 13 (8), e0202168. https://doi.org/10.1371/journal.pone.0202168.
Livak, K.J., Schmittgen, T.D., 2001. Analysis of relative gene expression data using real-time quantitative PCR and the $2^{-\Delta\Delta C_T}$ method. Methods 25 (4), 402–408. https://doi.org/10.1006/meth.2001.1262.
Los, D.A., Mironov, K.S., Allakhverdiev, S.I., 2013. Regulatory role of membrane fluidity in gene expression and physiological functions. Photosynth. Res. 116, 489–509. https://doi.org/10.1007/s11120-013-9823-4.
Moellering, E.R., Muthan, B., Benning, C., 2010. Freezing tolerance in plants requires lipid remodeling at the outer chloroplast membrane. Science 330 (6001), 226–228. https://doi.org/10.1126/science.1191803.
Moon, B.Y., Higashi, S., Gombos, Z., Murata, N., 1995. Unsaturation of the membrane lipids of chloroplasts stabilizes the photosynthetic machinery against low-temperature photoinhibition in transgenic tobacco plants. Proc. Natl. Acad. Sci. U. S. A. 92 (14), 6219–6223. https://doi.org/10.1073/pnas.92.14.6219.
Murata, N., Ishizaki-Nishizawa, O., Higashi, S., Hayashi, H., Tasaka, Y., Nishida, I., 1992. Genetically engineered alteration in the chilling sensitivity of plants. Nature 356 (6371), 710–713. https://doi.org/10.1038/356710a0.
Nishiyama, Y., Murata, N., 2014. Revised scheme for the mechanism of photoinhibition and its application to enhance the abiotic stress tolerance of the photosynthetic machinery. Appl. Microbiol. Biotechnol. 98 (21), 8777–8796. https://doi.org/10.1007/s00253-014-6020-0.
Romero-Puertas, M.C., Rodríguez-Serrano, M., Corpas, F.J., Gomez, M., Delrio, L.A., Sandalio, L.M., 2004. Cadmium-induced subcellular accumulation of O_2^- and H_2O_2 in pea leaves. Plant Cell Environ. 27 (9), 1122–1134. https://doi.org/10.1111/j.1365-3040.2004.01217.x.
Sakamoto, A., Sulpice, R., Hou, C.X., Kinoshita, M., Higashi, S.I., Kanaseki, T., Nonaka, H., Moon, B.Y., Murata, N., 2003. Genetic modification of the fatty acid unsaturation of phosphatidylglycerol in chloroplasts alters the sensitivity of tobacco plants to cold stress. Plant Cell Environ. 27 (1), 99–105. https://doi.org/10.1046/j.0016-8025.2003.01131.x.
Sheng, X., Liu, X., Cao, P., Li, M., Liu, Z., 2018. Structural roles of lipid molecules in the assembly of plant PSII-LHCII supercomplex. Biophys. Rep. 4 (4), 189–203. https://doi.org/10.1007/s41048-018-0068-9.
Shi, Y., Ding, Y., Yang, S., 2018. Molecular regulation of CBF signaling in cold acclimation. Trends Plant Sci. 23 (7), 623–637. https://doi.org/10.1016/j.tplants.2018.04.002.
Siegenthaler, P.A., Eichenberger, W., 1984. Structure, function, and metabolism of plant lipids. 9. Elsevir, Amsterdam, pp. 16–20.
Sui, N., Li, M., Liu, X.Y., Wang, N., Fang, W., Meng, Q.W., 2007a. Response of xanthophyll cycle and chloroplastic antioxidant enzymes to chilling stress in tomato over-expressing glycerol-3-phosphate acyltransferase gene. Photosynthetica 45 (3), 447–454. https://doi.org/10.1007/s11099-007-0074-5.
Sui, N., Li, M., Shu, D.F., Zhao, S.J., Meng, Q.W., 2007b. Antisense-mediated depletion of tomato chloroplast glycerol-3-phosphate acyltransferase affects male fertility and increases thermal tolerance. Physiol. Plant 130 (2), 301–314. https://doi.org/10.1111/j.1399-3054.2007.00907.x.
Sui, N., Li, M., Zhao, S.J., Li, F., Liang, H., Meng, Q.W., 2007c. Overexpression of glycerol-3-phosphate acyltransferase gene improves chilling tolerance in tomato. Planta 226 (5), 1097–1108. https://doi.org/10.1007/s00425-007-0554-7.
Sui, N., Tian, S., Wang, W.Q., Wang, M.J., Fan, H., 2017. Overexpression of glycerol-3-phosphate acyltransferase from *Suaeda salsa* improves salt tolerance in Arabidopsis. Front. Plant Sci. 8, 1337. https://doi.org/10.3389/fpls.2017.01337.
Sun, S.K., Yang, N.N., Chen, L.J., Irfan, M., Zhao, X.H., Li, T.L., 2015. Characterization of LpGPAT gene in *Lilium pensylvanicum* and response to cold stress. BioMed Res. Int. 2015, 792819. https://doi.org/10.1155/2015/792819.
Sun, X.L., Yang, S., Wang, L.Y., Zhang, Q.Y., Zhao, S.J., Meng, Q.W., 2011. The unsaturation of phosphatidylglycerol in thylakoid membrane alleviates PSII photoinhibition under chilling stress. Plant Cell Rep. 30 (10), 1939–1947. https://doi.org/10.1007/s00299-011-1102-2.
Sun, Y.L., Li, F., Su, N., Sun, X.L., Zhao, X.J., Meng, Q.W., 2010. The increase in unsaturation of fatty acids of phosphatidylglycerol in thylakoid membrane enhanced salt tolerance in tomato. Photosynthetica 48 (3), 400–408. https://doi.org/10.1007/s11099-010-0052-1.
Tamada, T., Feese, M.D., Ferri, S.R., Kato, Y., Yajima, R., Toguri, T., Kurok, R., 2004. Substrate recognition and selectivity of plant glycerol-3-phosphate acyltransferases (GPATs) from *Cucurbita moscata* and *Spinacea oleracea*. Acta Crystallogr. D Biol. Crystallogr. 60 (1), 13–21. https://doi.org/10.1107/s0907444903020778.
Upchurch, R.G., 2008. Fatty acid unsaturation, mobilization, and regulation in the response of plants to stress. Biotechnol. Lett. 30 (6), 967–977. https://doi.org/10.1007/s10529-008-9639-z.
Wada, H., Murata, N., 2007. The essential role of phosphatidylglycerol in photosynthesis. Photosynth. Res. 92 (2), 205–215. https://doi.org/10.1007/s11120-007-9203-z.
Wallis, J.G., Browse, J., 2002. Mutants of Arabidopsis reveal many roles for membrane lipids. Progress in Lipid Research 41 (3), 254–278. https://doi.org/10.1016/s0163-7827(01)00027-3.
Waschburger, E., Kulcheski, F.R., Veto, N.M., Marqis, R., Marqis-Pinheiro, M., Turchetto-Zolet, A.C., 2018. Genome-wide analysis of the glycerol-3-phosphate acyltransferase (GPAT) gene family reveals the evolution and diversification of plant GPATs. Genet. Mol. Biol. 41 (1 Suppl. 1), 355–370. https://doi.org/10.1590/1678-4685-GMB-2017-0076.
Wu, Y.Q., Wei, W., Pang, X.Y., Wang, X.F., Zhang, H.L., Dong, B., Xing, Y.P., Li, X.G., Wang, M.Y., 2014. Comparative transcriptome profiling of a desert evergreen shrub, *Ammopiptanthus mongolicus*, in response to drought and cold stresses. BMC Genomics 15 (1), 671. https://doi.org/10.1186/1471-2164-15-671.
Xu, Y., Siegenthaler, P.A., 1997. Low temperature treatments induce an increase in the relative content of both linolenic and Δ^3-*trans*-hexadecenoic acids in thylakoid membrane phosphatidylglycerol of squash cotyledons. Plant Cell Physiol. 38 (5), 611–618. https://doi.org/10.1093/oxfordjournals.pcp.a029211.
Xu, C., Yu, B., Cornish, A.J., Froehlich, J.E., Benning, C., 2006. Phosphatidylglycerol biosynthesis in chloroplasts of Arabidopsis mutants deficient in acyl-ACP glycerol-3-phosphate acyltransferase. Plant J. 47 (2), 296–309. https://doi.org/10.1111/j.1365-313X.2006.02790.x.
Yan, K., Chen, N., Qu, Y.Y., Dong, X.C., Meng, Q.W., Zhao, S.J., 2008. Overexpression of sweet pepper glycerol-3-phosphate acyltransferase gene enhanced thermotolerance of photosynthetic apparatus in transgenic tobacco. J. Integr. Plant Biol. 50 (5), 613–621. https://doi.org/10.1111/j.1744-7909.2008.00652.x.
Yin, Y.M., Jiang, X.X., Ren, M.Y., Xue, M., Nan, D., Wang, Z.L., Xing, Y.P., Wang, W.Y., 2018. *AmDREB2C*, from *Ammopiptanthus mongolicus*, enhances abiotic stress tolerance and regulates fatty acid composition in transgenic *Arabidopsis*. Plant Physiol. Biochem. 130, 517–528. https://doi.org/10.1016/j.plaphy.2018.08.002.
Yokoi, S., Higashi, S.I., Kishitani, S., Murata, N., Toriyama, K., 1998. Introduction of the cDNA for shape Arabidopsis glycerol-3-phosphate acyltransferase (GPAT) confers unsaturation of fatty acids and chilling tolerance of photosynthesis on rice. Mol. Breed. 4 (3), 269–275. https://doi.org/10.1023/a:1009671231614.